Journal of Archaeological Science xxx (2012) 1–14

Contents lists available at SciVerse ScienceDirect

Journal of Archaeological Science

journal homepage: http://www.elsevier.com/locate/jas

Observatory validation of Neolithic tells ("Magoules") in the Thessalian plain, central Greece, using hyperspectral spectroradiometric data

Athos Agapiou [a,*], Diofantos G. Hadjimitsis [a], Dimitrios Alexakis [a], Apostolos Sarris [b]

[a] Department of Civil Engineering and Geomatics, Faculty of Engineering and Technology, Cyprus University of Technology, 2-6, Saripolou str., 3603 Limassol, Cyprus
[b] Laboratory of Geophysical – Satellite Remote Sensing and Archaeo-environment, Institute for Mediterranean Studies, Foundation for Research & Technology, Hellas (F.O.R.T.H.), 130, Nikiforou Foka str., 74100 Rethymno, Crete, Greece

ARTICLE INFO

Article history:
Received 2 September 2011
Received in revised form
28 December 2011
Accepted 3 January 2012

Keywords:
Remote sensing archaeology
Ground spectroradiometic data
Vegetation indices
Detection archaeological sites
Crop marks

ABSTRACT

This paper presents the results obtained from field spectroradiometric campaigns over Neolithic tells ("magoules") located at the Thessalian region in Greece. In each one of the four archaeological sites selected, three sections were carried out using the GER 1500 handheld spectroradiometer. Spectral profiles of the sections and several vegetation indices such as Normalized Difference Vegetation Indices (NDVI) and Simple Ratio (SR) have been examined in this study. This is one of the first times that ground hyperspectral data are evaluated in such context of archaeological research for the spectral characterization of archaeological features. As it was found, ground spectroradiometric measurements can be efficiently used in order to support and validate satellite imagery results for the detection of archaeological sites.

1. Introduction

Remote sensing techniques have been widely used for the detection of archaeological sites (Rowlands and Sarris, 2007; Masini and Lasaponara, 2007). Such techniques include the use of geophysical surveys through the employment of ground penetrating radars and magnetometers (Ventera et al., 2006; Negria and Leucci, 2006), while other techniques involve the use of aerial (oblique or vertical) and satellite imagery (Cavalli et al., 2007; Parcak, 2009).

Several researchers have shown that high resolution satellite sensors can have a significant potential for archaeological investigations. The majority of these studies focused on the use of high resolution satellite imagery like IKONOS and QuickBird (Altaweel, 2005; Lasaponara and Masini, 2005, 2006, 2007). Hyperspectral satellite images such as HYPERION and MIVIS have been found to be suitable for retrieving valuable information in an archaeological context revealing buried architectural remains (Traviglia, 2005; Aqdus et al., 2007, 2008; Bassani et al., 2009).

However, in most of these studies there is lack of ground verification from satellite investigations. Satellite images need to be atmospherically and geometrically corrected, before being subjected to any post-processing techniques (Lillesand et al., 2004). Other corrections taken into account are sun elevation, elevation of the area of interest e.t.c (Campbell, 2002). Within ground surveys, in situ spectroradiometric can provide more accurate results (ground "truth" data) regarding the reflectance of each target. These instruments measure the amount of energy (radiance) reflected from a ground area for a range of wavelengths and then these measurements can be converted to reflectance values using calibrated spectralon panels (Peddle et al., 2001). Therefore spectroradiometers can be used for measuring the canopy reflectance over areas with archaeological interest. Spectral data are typically obtained for small areas at ground level (as the case of this paper) or from tower platforms in a variety of configurations (e.g. field of view, height, angle, etc) using portable field spectroradiometers.

Peddle et al. (2001) argue that field measurements of surface reflectance, using spectroradiometers, have been already applied in a number of remote sensing approaches such as vegetation canopy reflectance modeling, spectral mixture analysis, classification techniques or even predictive modeling.

Field spectroscopy involves not only the acquisition of accurate measurements but also the study of the interrelationships between the spectral characteristics of objects and their biophysical

* Corresponding author.
E-mail addresses: athos.agapiou@cut.ac.cy (A. Agapiou), d.hadjimitsis@cut.ac.cy (D.G. Hadjimitsis), dimitrios.alexakis@cut.ac.cy (D. Alexakis), asaris@ret.forthnet.gr (A. Sarris).

0305-4403/$ – see front matter © 2012 Elsevier Ltd. All rights reserved.
doi:10.1016/j.jas.2012.01.001

Table 1
Vegetation indices used in the spectroradiometric study of the Thessalian magoules.

Equation no.	Vegetation index	Equation	Reference
1	NDVI (Normalized Difference Vegetation Index)	$(p_{NIR} - p_{red})/(p_{NIR} + p_{red})$	Rouse et al. (1974)
2	SR (Simple Ration)	p_{NIR}/p_{red}	Jordan (1969)
3	Green NDVI (Green Normalized Difference Vegetation Index)	$(p_{NIR} - p_{green})/(p_{NIR} + p_{green})$	Gitelson et al., 1996
4	EVI (Enhanced Vegetation Index)	$2.5(p_{NIR} - p_{red})/(p_{NIR} + 6p_{red} - 7.5p_{blue} + 1)$	Huete et al., 1997
5	SAVI (Soil adjusted Vegetation Index)	$(1 + 0.5)(p_{NIR} - p_{red})/(p_{NIR} + p_{red} + 0.5)$	Huete, 1988
6	ARVI (Atmospherically Resistant Vegetation Index)	$(p_{NIR} - p_{rb})/(p_{NIR} + p_{rb})$ $p_{rb} = p_{red} - \gamma(p_{blue} - p_{red})$	Kaufman and Tanré, 1992
7	SARVI (Soil and Atmospherically Resistant Vegetation Index)	$(1 + 0.5)(p_{NIR} - p_{rb})/(p_{NIR} - p_{rb} + 0.5)$ $p_{rb} = p_{red} - \gamma(p_{blue} - p_{red})$	Kaufman and Tanré, 1992
8	GEMI (Global Environment Monitoring Index)	$n(1 - 0.25n)(p_{red} - 0.125)/(1 - p_{red})$ $n = \left[2\left(p_{NIR}^2 - p_{red}^2\right) + 1.5p_{NIR} + 0.5p_{red}\right] / (p_{NIR} + p_{red} + 0.5)$	Pinty and Verstraete, 1992
9	MSR (Modified Simple Ratio)	$p_{red}/[(p_{NIR}/p_{red} + 1)]^{1/2}$	Chen, 1996
10	PVI (Perpendicular Vegetation Index)	$(p_{NIR} - \alpha p_{red} - b)/(1 + \alpha^2), p_{NIR,soil}\alpha p_{red,soil} + b$	Richardson and Wiegand, 1977
11	TSAVI (Transformed Soil Adjusted Vegetation Index)	$[\alpha(p_{NIR} - \alpha p_{NIR} - b)]/[(p_{red} + \alpha p_{NIR} - \alpha b + 0.08(1 + \alpha^2))]$ $p_{NIR,soil}\alpha p_{red,soil} + b$	Baret and Guyot, 1991
12	OSAVI (Optimized Soil Adjusted Vegetation Index)	$(p_{NIR} - p_{red})/(p_{NIR} + p_{red} + 0.16)$	Rondeaux et al., 1996
13	MSAVI (Modified Soil Adjusted Vegetation Index)	$[2p_{NIR} + 1 - [(2p_{NIR} + 1)^2 - 8(p_{NIR} - p_{red})]^{1/2}]/2$	Qi et al., 1994
14	RDVI (Renormalized Difference Vegetation Index)	$(p_{NIR} - p_{red})/(p_{NIR} + p_{red})^{1/2}$	Roujean and Breon, 1995
15	DVI (Difference Vegetation Index)	$p_{NIR} - p_{red}$	Tucker, 1979

p_{NIR} is the near infrared reflectance.
p_{red} is the red reflectance.
p_{green} is the green reflectance.
p_{blue} is the blue reflectance.

attributes in the field environment (Milton, 1987). Therefore, field spectroscopy can provide valuable information for an area if we consider the fact that human eye senses only a small part of the electromagnetic spectrum, from approximately 400 to 700 nm, whereas field spectroscopy in support of remote sensing operates in a wider spectral range to including the near infrared.

This paper presents field campaign results obtained from the Thessalian plain in central Greece where known archaeological sites in the form of tells (called "magoules") are located. These data were acquired from a GER 1500 field spectroradiometer covering a range from 400 nm–1050 nm. Such data may give accurate spectral reflectance results, minimizing any potential errors of the at satellite reflectance. The aim of this study was to analyze spectral ground data from wheat canopy and to examine their response in presence of the archaeological sites.

Using spectroradiometers, researchers can evaluate if Vegetation Indices (e.g. NDVI) are able to discriminate archaeological sites from the surrounding area, in a similar way as it has been applied to distinguish different types of canopy or cultivation crops. Vegetation indices have already been used and applied for the detection of archaeological crop marks in different areas (e.g. Rowlands and Sarris, 2007; Masini and Lasaponara, 2007; Cavalli et al., 2007; Parcak, 2009; Lasaponara and Masini, 2005, 2006, 2007; Aqdus et al., 2007, 2008; Bassani et al., 2009). For example, Masini and Lasaponara (2007) showed that the usage of Quickbird multispectral data can be very promising in order to reconstruct the shape of buried remains. In addition, it was proved that spectral differences, in vegetated areas, linked to the presence of ancient buried structures were better emphasized in the near infrared (NIR) band. Aqdus et al. (2008) came to the same conclusion by using hyperspectral data.

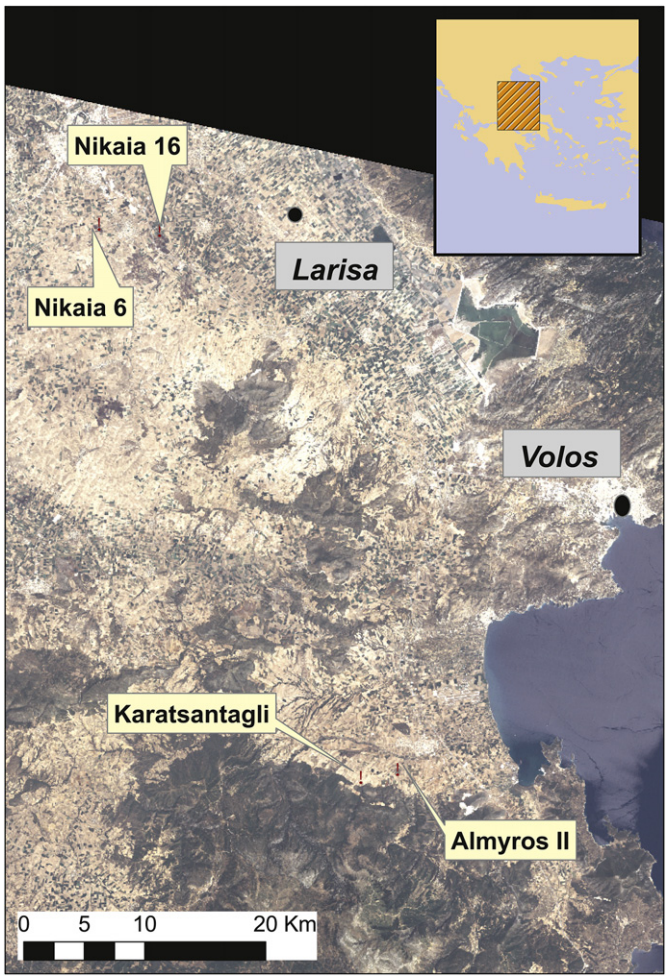

Fig. 1. Map of the archaeological sites (magoules) mentioned in the paper.

2. Vegetation indices

Vegetation indices are usually employed in order to monitor seasonal or even long-term variations of structural, phenological

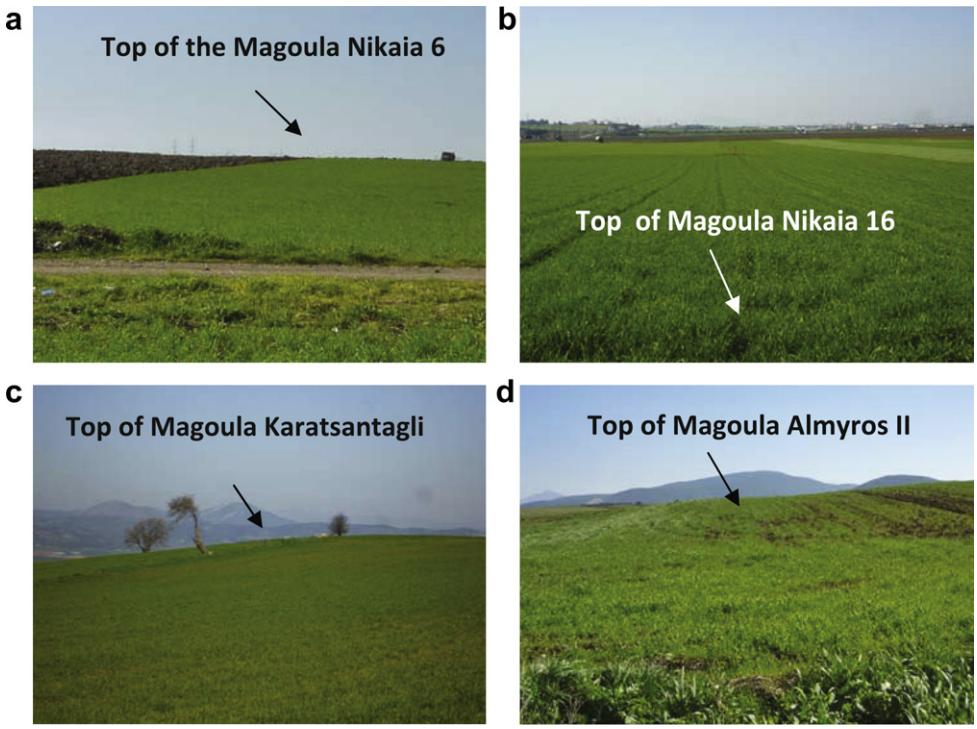

Fig. 2. View from: a) Nikaia 6, b) Nikaia 16, c) Karatsantagli and d) Almyros II archaeological site.

and biophysical parameters of land surface vegetation cover (Aqdus et al., 2007; Bassani et al., 2009). These indices are quantitative measures, based on vegetation spectral properties that attempt to measure biomass or vegetative vigor (Jackson and Huete, 1991). Theoretical analyses and field studies have shown that vegetation indices are near-linearly related to photosynthetically active plants which absorb radiation, and therefore to light-dependent physiological processes (e.g. photosynthesis), occurring in the upper canopy (Glenn et al., 2008).

NDVI is the most known vegetation index used for archaeological purposes. It was first developed by Rouse et al. (1974) and since then it was applied in several applications including the detection or monitoring of archaeological sites (e.g. Hadjimitsis et al., 2009). Simple Ratio (SR) index was firstly developed by Jordan (1969) and uses the characteristic curve of vegetation canopies at the red and near infrared spectrum (red edge). In the last years further vegetation indices were developed in order to minimized either atmospheric effects such as ARVI (Kaufman and Tanré, 1992), GEMI (Pinty and Verstraete, 1992) and EVI (Huete et al., 1997), or soil background effects like SAVI (Huete, 1988), TSAVI (Baret and Guyot, 1991), OSAVI (Rondeaux et al., 1996) and MSAVI (Qi et al., 1994) or even to minimize both effects such as SARVI (Kaufman and Tanré, 1992) (see Table 1 for indices equations). Furthermore other indices were developed in order to monitor specific plant characteristics like the Green NDVI index which is more sensitive to Chl-a concentrations by 5 times more than the NDVI (Gitelson et al., 1996). Due to the numerous data collected in the field campaigns at the Thessalian plain (see Chapter 3), this study presents the results of the first two indices (NDVI and SR) which are widely applied for the detection of archaeological sites using multispectral satellite images (Lasaponara and Masini, 2007; Masini and Lasaponara, 2007; Rowlands and Sarris, 2007; Agapiou and Hadjimitsis, 2011), while for the other indices (see Table 1), only some characteristic results are presented (further results can be found in the Supplementary information of the study).

3. Case study area

The Thessalian region is located in central Greece and it is considered as the primary agricultural area of Greece. At this plain many of Neolithic settlements/tells called magoules were established from the Early Neolithic period until the Bronze Age (6000–3000 BC). The magoules are typically low hills of 1–5 m height and they mainly consist of loam and mud based materials. Hundreds of magoules are located all over Thessaly and can be found within different kinds of vegetation. Due to the intensive cultivation of the land in the past and their low elevation, a major number of them are not clearly visible from the ground (Alexakis et al., 2009, 2011).

The period between mid October until mid of May is preferred for the detection of possible crop marks (barley and wheat) over known archaeological sites using remote sensing techniques and spectroradiometric measurements. During this period the

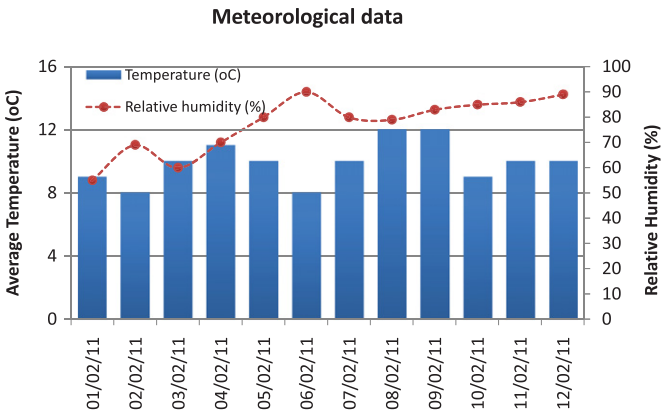

Fig. 3. Meteorological data from Larissa meteorological station (average temperature and average relative humidity).

Please cite this article in press as: Agapiou, A., et al., Observatory validation of Neolithic tells ("Magoules") in the Thessalian plain, central Greece, using hyperspectral spectroradiometric data, Journal of Archaeological Science (2012), doi:10.1016/j.jas.2012.01.001

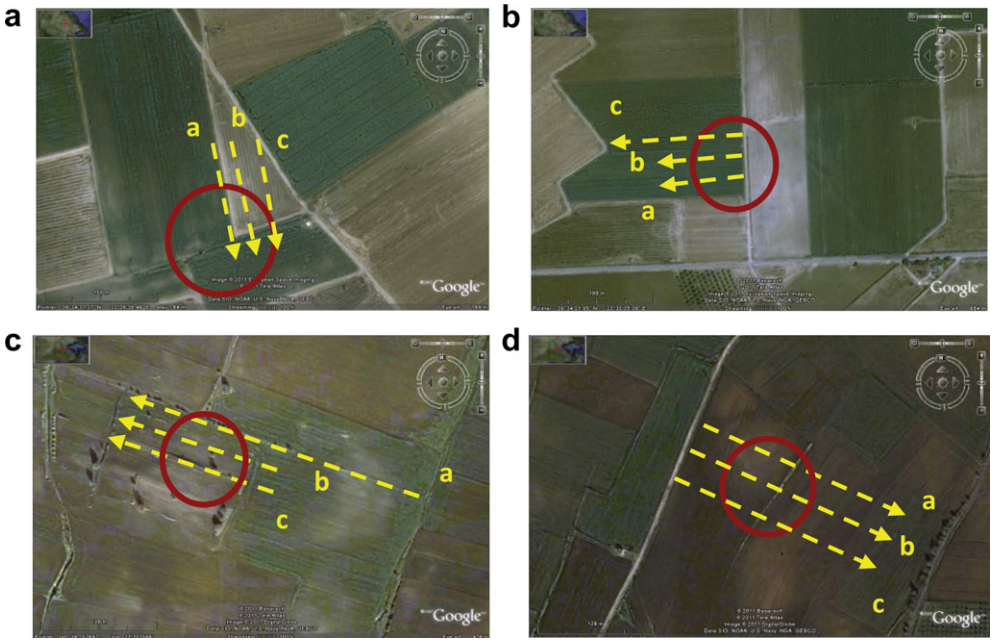

Fig. 4. Visible relief of the magoula (in red circle) and measurements taken as cross sections (yellow dash line): a) Nikaia 6, b) Nikaia 16, c) Karatsantagli and d) Almyros II (base map from Google Earth©). (For interpretation of the references to color in this figure legend, the reader is referred to the web version of this article.)

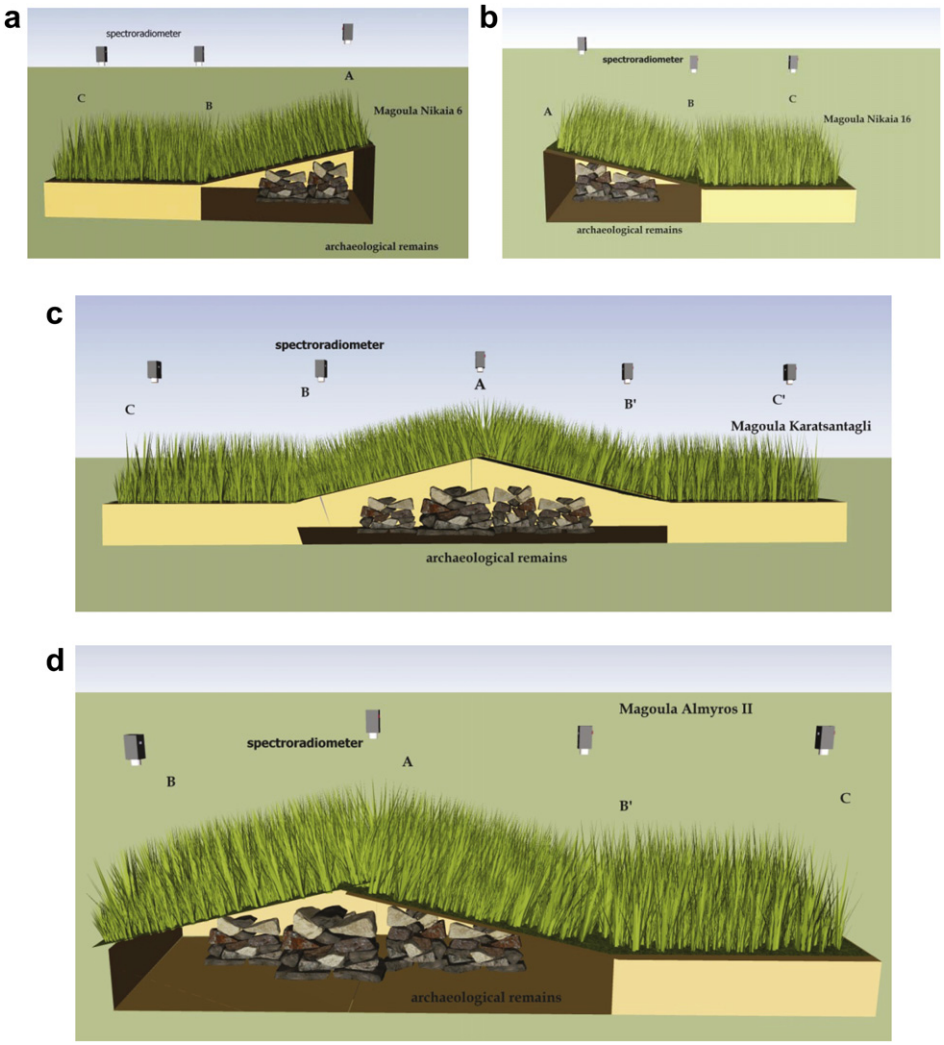

Fig. 5. Sketch of the profile of the section over the archaeological sites (a: Nikaia 6, b: Nikaia 16, c: Karatsantagli and d: Almyros II). Point *C* corresponds to the flat cultivated area, Point *B* to the beginning of the slope of the Magoula while Point *A* to the highest point of the site.

Please cite this article in press as: Agapiou, A., et al., Observatory validation of Neolithic tells ("Magoules") in the Thessalian plain, central Greece, using hyperspectral spectroradiometric data, Journal of Archaeological Science (2012), doi:10.1016/j.jas.2012.01.001

vegetation is grown (high Leaf Area Index) and background soil reflectance effect is minimized.

Alexakis et al. (2009, 2011) have recently examined this area using multispectral and hyperspectral images. Different algorithms were assessed for enhancement of archaeological sites, while spatial filters were examined for the detection of the low reliefs from various Digital Elevation Models. These studies reached the conclusion that magoules can be detected using the at satellite reflectance during specific periods of time.

This particular study is focused on four magoules named: Nikaia 6, Nikaia 16, Karatsantagli and Almyros II (Fig. 1). The first three sites are relatively visible in the low relief landscape of the Thessalian plain while the last site is not such clearly visible (Fig. 2). During the time of the field campaign for the collection of spectroradiometric measurements all the archaeological sites were cultivated with wheat crops.

Nikaia 6 and Nikaia 16 are dated to the Late Neolithic period and they are located in a hilly area, approximately 1.5 km from the modern settlement of Nikaia. The magoules have a circular shape with diameter of about 120 m (Nikaia 6) and 150 m (Nikaia 16) and they stand at a height of 2 m above the surrounding area (Galli, 1992).

Karatsantagli settlement is dated to the Early and Middle Neolithic Period and it is considered to be the earliest site in the region. The site is estimated to be less than 8 acres while a high density of ceramics were found at the top of the Karatsantagli site during a recent archaeological surface survey (more than 20–25 ceramics/m^2) (see Vouzaksakis, 2009). Recently, Almyros II

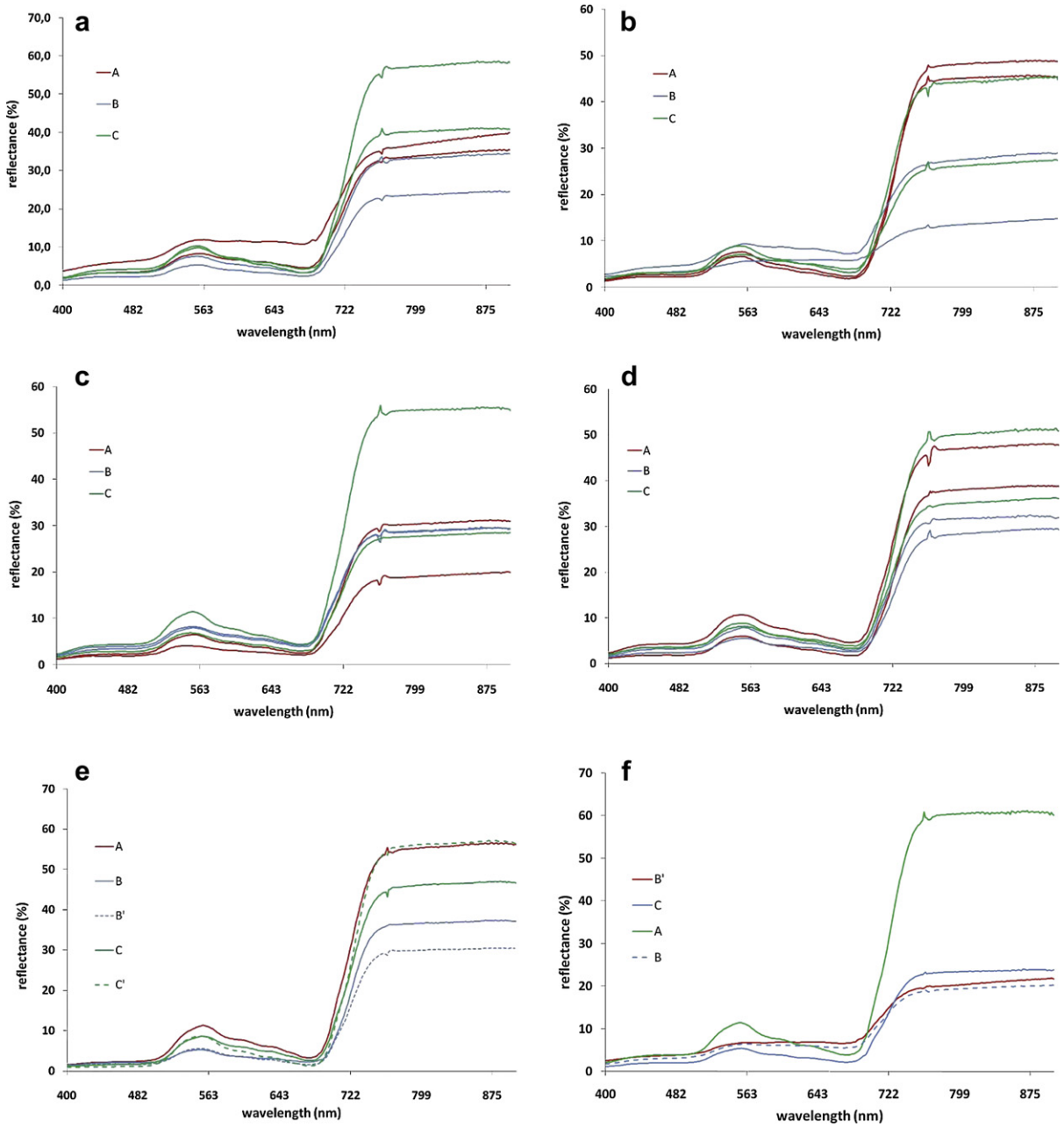

Fig. 6. Spectral profiles from spectroradiometer over the archaeological sites (a: for section a of Nikaia 6, b: for section b of Nikaia 6, c: for section c of Nikaia 6, d: for section c of Nikaia 16, e: for section b of Karatsantagli, and f: for section b of Almyros II). Points *C* and *C′* correspond to the flat cultivated area, Points *B* and *B′* to the beginning/end of the slope of the Magoula, while Point *A* to the highest point of the site.

Please cite this article in press as: Agapiou, A., et al., Observatory validation of Neolithic tells ("Magoules") in the Thessalian plain, central Greece, using hyperspectral spectroradiometric data, Journal of Archaeological Science (2012), doi:10.1016/j.jas.2012.01.001

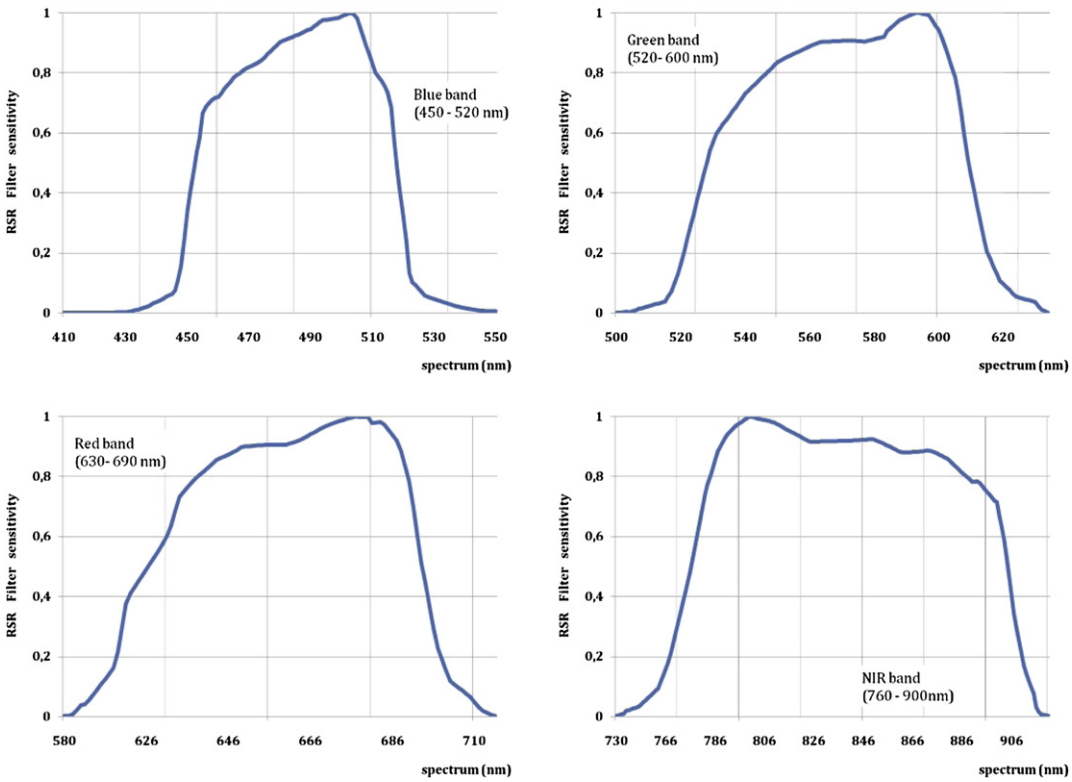

Fig. 7. RSR filters of Landsat 5 for Bands 1–4.

site was also surveyed and the results showed a high density of ceramics at the top of the magoula ($\approx$10 ceramics/m^2).

The climatic data (Fig. 3) provided from the meteorological station of Larisa (see Fig. 1) shows that the average temperature and the relative humidity was stable for at least two weeks prior to the field campaign while at the same time the precipitation was 0.0 mm for all days. It should be mentioned that the meteorological station of Volos (see Fig. 1) has also recorded very similar climatic data. Therefore vegetation, at the case study area, was not exposed to any stress conditions (e.g. water stress).

4. Methodology and data collection

GER 1500 spectroradiometer was used for the collection of spectral profiles over the archaeological sites in the Thessalian plain. This instrument has the capability to record the reflectance from 400 nm up to 1050 nm (blue/green/red and NIR band) while the spatial resolution of each measurement was estimated up to 0.02 m^2. A calibrated spectralon panel was used in order to minimize illumination errors during the data collection. Moreover, the GNSS Leica Global Positioning System (GPS) was also used for

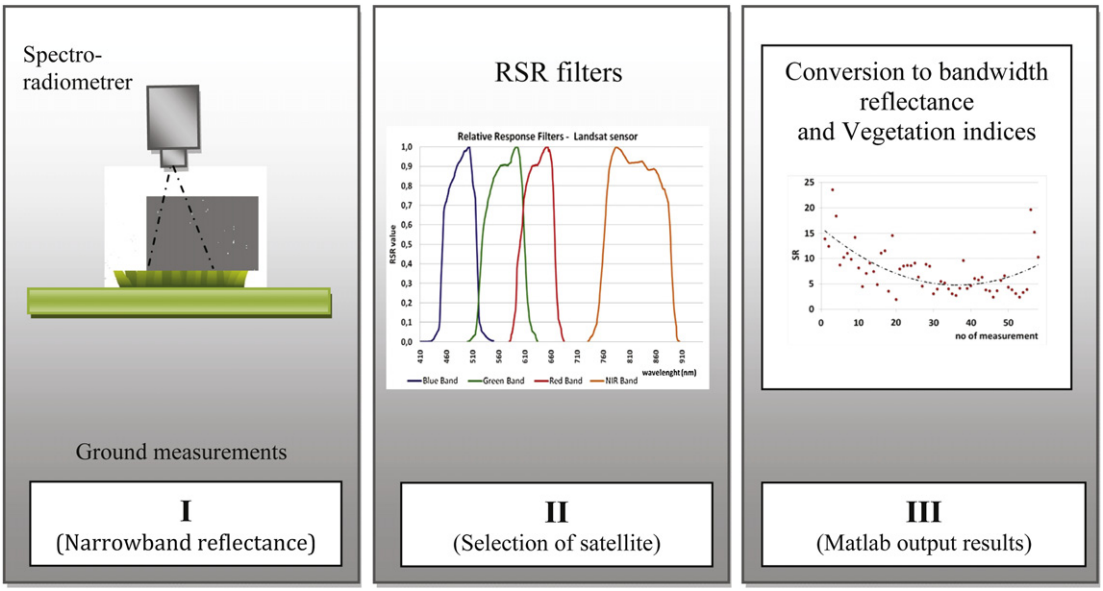

Fig. 8. Broadband reflectance from narrow bands of spectroradiometer.

Please cite this article in press as: Agapiou, A., et al., Observatory validation of Neolithic tells ("Magoules") in the Thessalian plain, central Greece, using hyperspectral spectroradiometric data, Journal of Archaeological Science (2012), doi:10.1016/j.jas.2012.01.001

geo-referencing the in situ measurements in a common coordinate system (WGS '84).

In each archaeological site three sections were carried out. Along each section, ground spectroradiometric measurements were taken from both sides of each magoula with the handheld instrument. More than 50 measurements were acquired in each section while in each consecutive 5th measurement the calibration spectralon panel was used in order to minimize sun changes illuminations (see Milton, 1987).

In detail, two field spectroradiometric campaigns were carried out on the 11th and 12th of February 2011 in all four archaeological sites. Spectroradiometric measurements were carried out between 10:00 and 14:00 (local time) in order to minimize the impact of illumination changes on the spectral responses (Milton, 1987). All the measurements were taken from nadir view, from a height of 1.2 m. In order to avoid vegetation's spectral differences due to different cultivation techniques, all measurements were carried out within the same parcel.

For magoula Nikaia 6, which was half cultivated with wheat crop – the other half was left uncultivated – three sections were carried out covering a distance of 200 m (Fig. 4a). The beginning of the sections was set up into a "healthy part" of the parcel while the end of each section was up to the highest peak of the magoula. Similarly with Nikaia 6, Nikaia 16 was half cultivated with wheat crop (Fig. 4b). The first two transects started over the magoula and continued to the healthy part of the parcel (flat region) covering a distance of approximately 130 m. However, the third one covered a distance of over 200 m. Measurements at the magoula Karatsantagli (Fig. 4c) – cultivated with wheat crops – were performed as follows: initially at the healthy part of the parcel then at the magoula itself and finally again at the healthy part of the magoula. The first transect covered a distance of 330 m while the next two transects covered a distance of 170 m. In Almyros II (Fig. 4d), three sections of approximately 150 m were carried out. The magoula was half cultivated and measurements were taken only in the west (cultivated) part of the magoula.

After the collection of the spectral data, the reflectance of each measurement was recalculated using the Relative Response Filters as done by other studies such as Papadavid et al. (2010) and Agapiou et al. (2011) (see Fig. 7). This procedure was performed automatically using an algorithm developed in Matlab environment. In this way the narrow reflectance bands of the spectroradiometer were converted into Landsat extensive band range (Band 1 to Band 4). Finally, vegetation indices (see Table 1) were

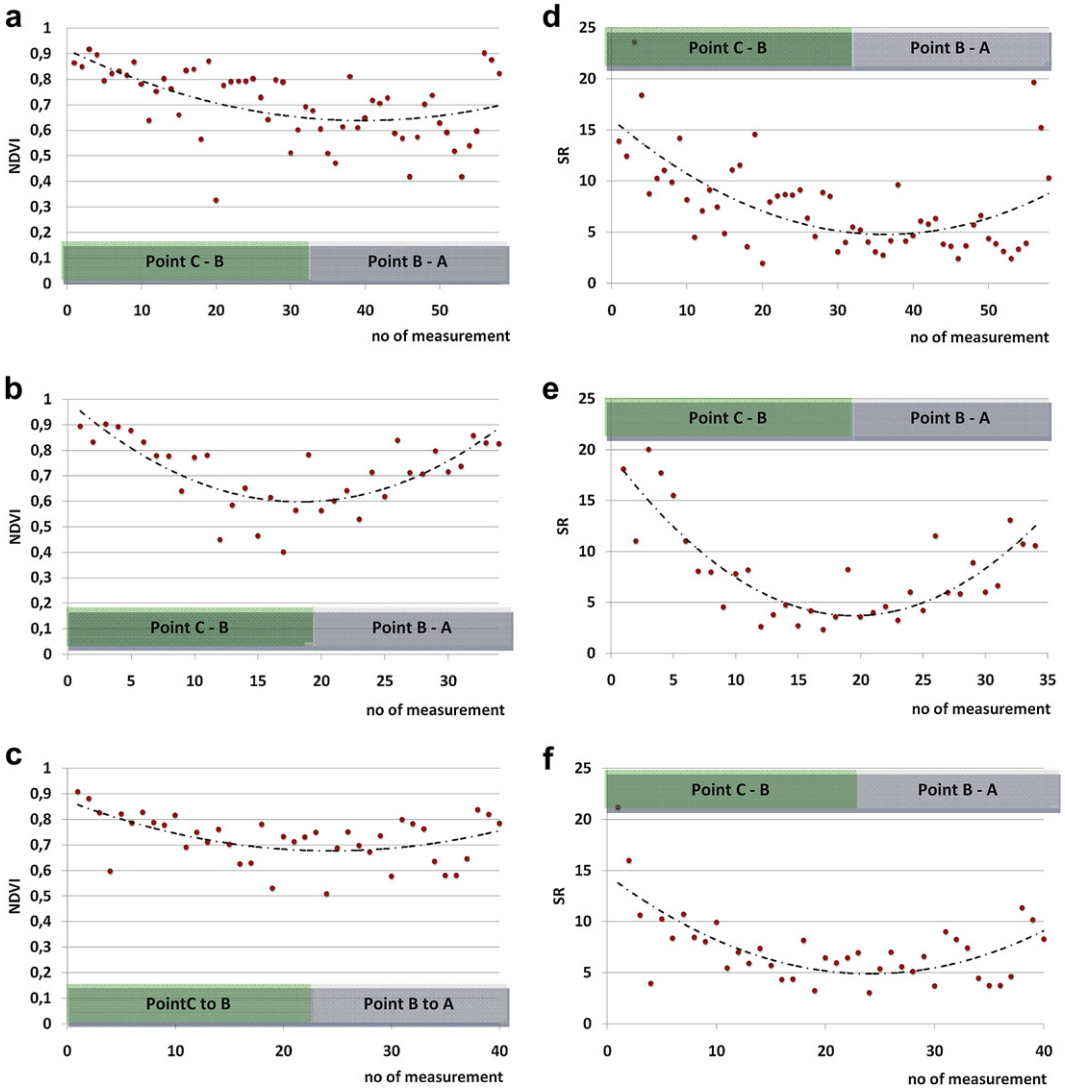

Fig. 9. NDVI (left) and SR (right) diagrams for the three transects (top to bottom) carried out in Nikaia 6 archaeological site. *X*-axis shows the number of measurements in each section while *Y*-axis indicated the NDVI value as calculated for every measurement.

Please cite this article in press as: Agapiou, A., et al., Observatory validation of Neolithic tells ("Magoules") in the Thessalian plain, central Greece, using hyperspectral spectroradiometric data, Journal of Archaeological Science (2012), doi:10.1016/j.jas.2012.01.001

calculated and plotted in diagrams in comparison with the relief profile of the section.

5. Results

5.1. Spectral profiles of the sections

The data collected from the in situ campaigns were analyzed using the SVC GER 1500 software. These data were archived based on acquisition date, site and the section, as were the reflectance profiles of the measurements to be plotted. Spectral profiles may be used in order to identify if vegetation stress (due to presence of archaeological sites) can be detected compared to non stress vegetation profiles. In this chapter, spectral profiles are presented for all archaeological sites studied in the paper. Due to the numerous measurements taken, only some typical examples of spectral profiles over characteristics points are analyzed.

In the case of Nikaia 6, each section can be divided by three Points *A*, *B* and *C*, which are the top of the magoula, the beginning of the magoula and a point of the flat area, respectively (see Fig. 5a).

Section a (Fig. 6a) has shown that vegetation in the flat region (Point *C*) tends to give highest reflectance values in the NIR spectrum (760–900 nm) whereas at the beginning of the slope of the magoula (Point *B*) this reflectance is minimized. At the highest peak of the magoula (Point *A*) the reflectance tends to get smaller (compared to the flat region – Point *C*) and similar signature response to Point *B*. Analogous results were extracted from the section c as well (Fig. 6c) since magoula can be distinguish from the flat vegetated region of the area. On the other hand, along section b (Fig. 6b) the highest peak of the magoula (Point *A*) has higher reflectance response compared to all the other measurements whereas the slope of the magoula (Point *B*) seems to be the most stress vegetated area. It should be mentioned that the second section was taken along the center of the magoula while the other two sections were carried out in about 10 m offset (left and right) from this central section.

Similar spectral profiles were observed for magoula Nikaia 16 (Fig. 5b) as well. Fig. 6d presents spectral profiles for section c. This section was carried out at the middle part of the magoula (the previous two sections were performed south to this section). The results were compatible to those of Nikaia 6, with Point *A* and Point *C* having similar spectral response whereas in Point *B* the measurements indicate some stress condition of vegetation.

At Karatsantagli magoula, measurements were taken from both sides of the magoula relief, since the entire parcel was cultivated. Therefore five characteristic points were measured with the GPS

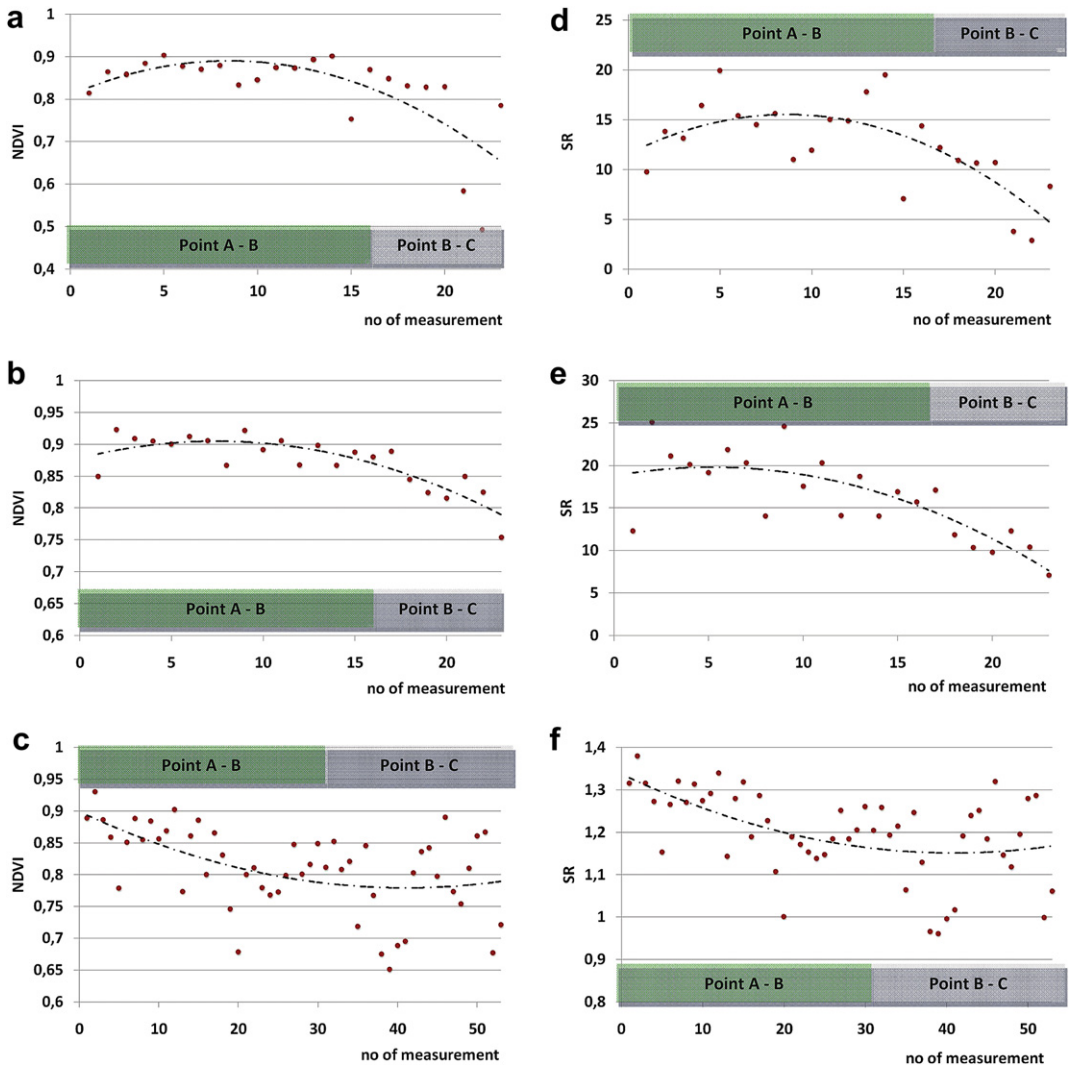

Fig. 10. NDVI (left) and SR (right) diagrams for the three transects (top to bottom) carried out in Nikaia 16 archaeological site. *X*-axis shows the number of measurements in each section while *Y*-axis indicated the NDVI value as calculated for every measurement.

Please cite this article in press as: Agapiou, A., et al., Observatory validation of Neolithic tells ("Magoules") in the Thessalian plain, central Greece, using hyperspectral spectroradiometric data, Journal of Archaeological Science (2012), doi:10.1016/j.jas.2012.01.001

system: Points *C* and *C′* corresponded to the flat areas before and after the peak of magoula relief, Points *B* and *B′* were over the beginning of the slope and at the end of the slope of the magoula while Point *A* was taken over the highest peak of the magoula (Fig. 5c). It is interesting to notice that Point *C* and Point *A* have the highest reflectance response in the NIR spectrum while Points *B* and *B′* have lower reflectance response than the peak of the magoula (Point *A*) (Fig. 6e).

Almyros II was also fully cultivated with wheat crops and thus measurements were carried out in a similar way to the magoula Karatsantagli. Four characteristic points were measured with the GPS system as indicated in Fig. 5d. The spectral profile of the canopy (Fig. 6f) denote the significant different response of the top of the magoula on the NIR compared to the healthy flat region of the parcel.

Comparing spectral diagrams from all the different archaeological sites it can be concluded that Point *B* and *B′* have a moderate reflectance response in the NIR spectrum compared to the highest peak of the magoula (Point *A*) and the flat part of each parcel (Point *C*). This observation is important since using NIR spectrum (e.g. Vegetation indices) one can potentially distinguish the main magoula from the healthy part which surrounds it. Moreover, it is recorded that for some sections (Nikaia 6 and Karatsantagli) NIR reflectance is higher at Point *A* compared to the healthy part of the parcel (Point *C*). This is the case when positive crops marks are identified using satellite images. Finally, Almyros II reflectance diagram is different from all the other magoula diagrams: similar reflectance response is observed for Point *C* and Point *B* (see Fig. 6f). This is probably due to the intensive cultivation of wheat crops at the magoula compared to the previous archaeological sites.

5.2. Vegetation indices

Spectral resolution of the GER 1500 spectroradiometer is approximately 1.5 nm. However, in order to examine the use of broadband vegetation indices such as NDVI, narrow band reflectance (from the spectroradiometer) needed to be recalculated according to the characteristics of a specific satellite sensor. The authors selected to simulate these data to Landsat 5 TM/7 ETM+ satellite imagery and therefore four bands were necessary to be calculated: band 1 (450–520 nm), band 2 (520–600 nm), band 3 (630–690 nm) and band 4 (760–900 nm).

For this reason, the Relative Spectral Response (RSR) filters of the Landsat sensor were used. RSR filters describe the instrument relative sensitivity to radiance at various part of the electromagnetic spectrum (Wu et al., 2010). Spectral responses have a value of

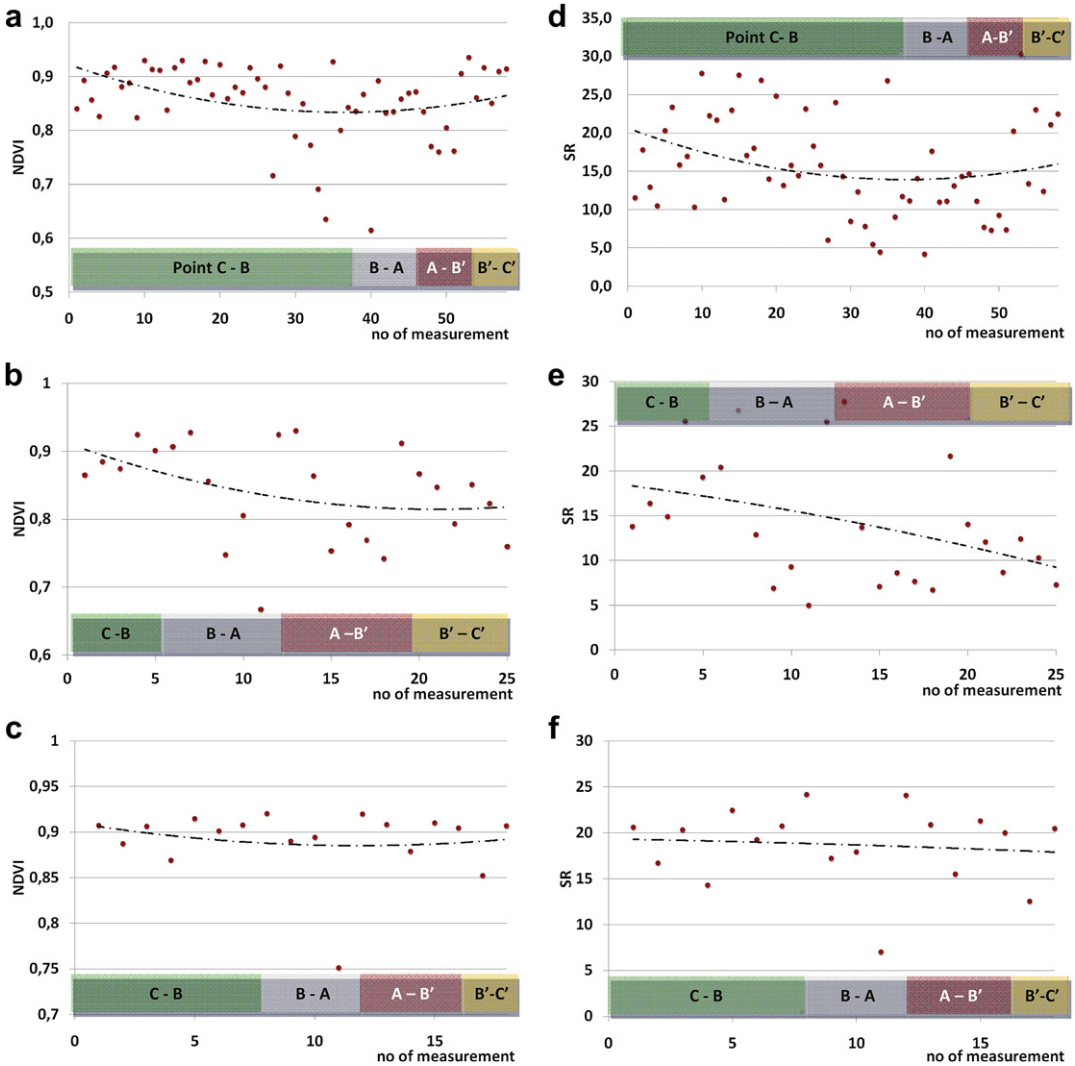

Fig. 11. NDVI (left) and SR (right) diagrams for the three transects (top to bottom) carried out in Karatsantagli archaeological site. *X*-axis shows the number of measurements in each section while *Y*-axis indicated the NDVI value as calculated for every measurement.

Please cite this article in press as: Agapiou, A., et al., Observatory validation of Neolithic tells ("Magoules") in the Thessalian plain, central Greece, using hyperspectral spectroradiometric data, Journal of Archaeological Science (2012), doi:10.1016/j.jas.2012.01.001

0–1 and have no units since they are relative to the peak response (Fig. 7). Bandpass filters are used in the same way in spectroradiometers in order to transmit a certain wavelength band, and block others. The reflectance from the spectroradiometer was calculated based on the wavelength of each sensor and the RSR filter as follows:

$$R_{band} = \sum(R_i * RSR_i) / \sum RSR_i \quad (16)$$

Where:

R_{band} = reflectance at a range of wavelength (e.g. Band 1)
R_i = reflectance at a specific wavelength (e.g. R_{450} nm)
RSR_i = Relative Response value at the specific wavelength.

An algorithm in the Matlab environment (the algorithm is freely distributed and presented in the Appendix), was developed, where the end-user can select the appropriate RSR file and the bands which are required to be recalculated (Fig. 8). Although the procedure is straight forward, Matlab environment can minimize random errors from end-users (e.g. instead of calculating band reflectance using spreadsheets) and can be easily expanded to any satellite sensor (both multispectral and hyperspectral) saving time in cases of hundreds of spectroradiometric measurements (similar to the case study presented in this paper).

After the necessary calculation of bands with the use of the RSR filter, the NDVI and the SR profile of each section was plotted. Moreover the other broadband indices mentioned in Table 1, are presented for the first section of Nikaia 6. Fig. 9a–c shows the NDVI profile for the sections a–c taken over Nikaia 6 magoula. A 2nd order polynomial best fit line was plotted using these measurements in order to show the overall trend of the data. As it was found, the NDVI values tend to get smaller at the lower relief of the magoula (Point *B*). This is more obvious in section b (central section over the magoula). In addition, NDVI values at the beginning and the end of the diagrams tend to be similar and very high (>0.9) which indicate a healthy vegetation. These values correspond to the values at the flat part of the parcel (Point *C*) and at the highest peak of the magoula (Point *A*). Simple Ratio diagrams concluded to similar results as indicated in Fig. 9d–f.

NDVI and SR profiles for the first two sections (a–b) over the magoula Nikaia 16 (Fig. 10a–f) show comparable results from Point *A* to Point *B* while moving to the flat area of the parcel the values tend to get smaller. Again the NDVI values, at Points *A* and *C*, as calculated from the spectroradiometric measurements, are very

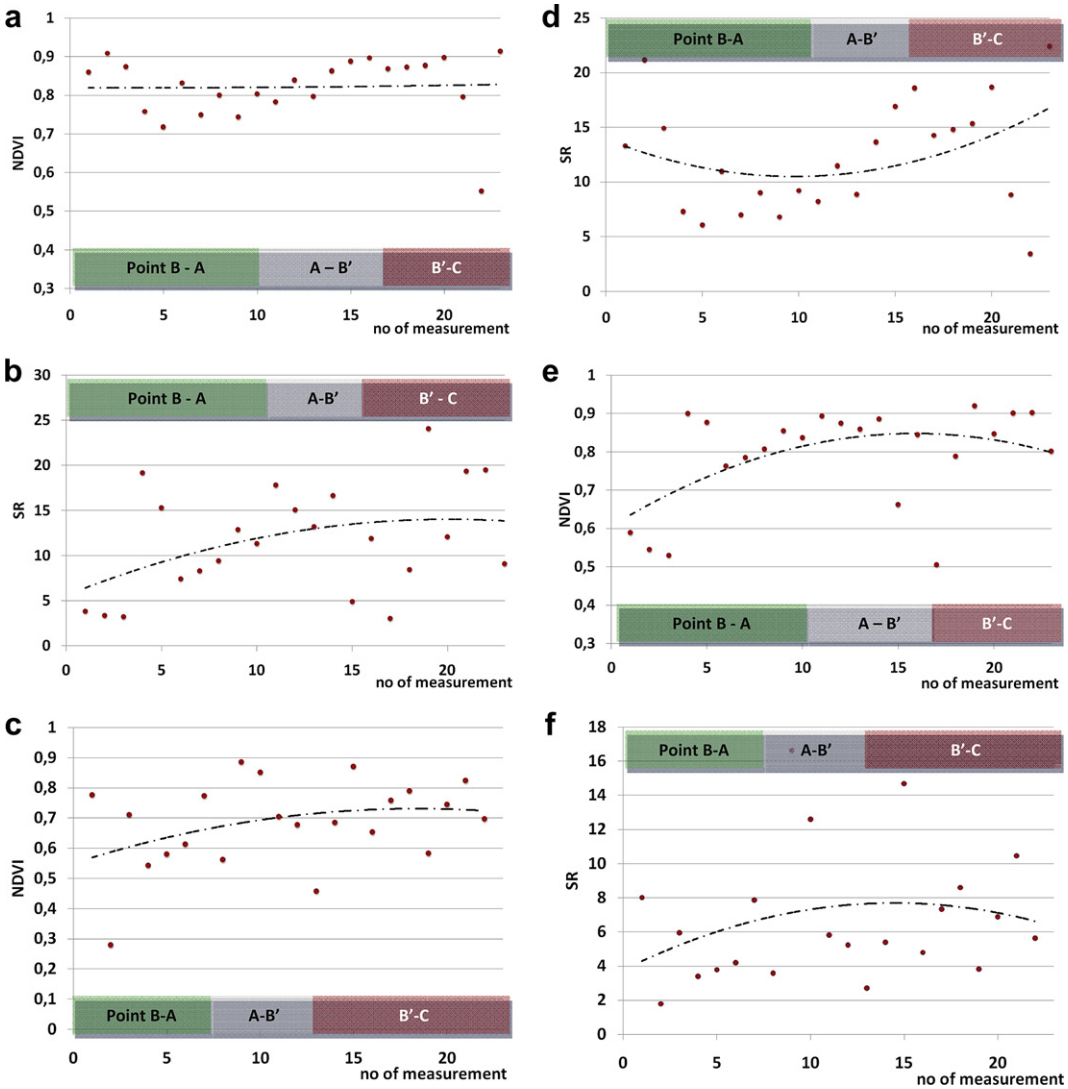

Fig. 12. NDVI (left) and SR (right) diagrams for the three transects (top to bottom) carried out in Almyros II archaeological site. *X*-axis shows the number of measurements in each section while *Y*-axis indicated the NDVI value as calculated for every measurement.

Please cite this article in press as: Agapiou, A., et al., Observatory validation of Neolithic tells ("Magoules") in the Thessalian plain, central Greece, using hyperspectral spectroradiometric data, Journal of Archaeological Science (2012), doi:10.1016/j.jas.2012.01.001

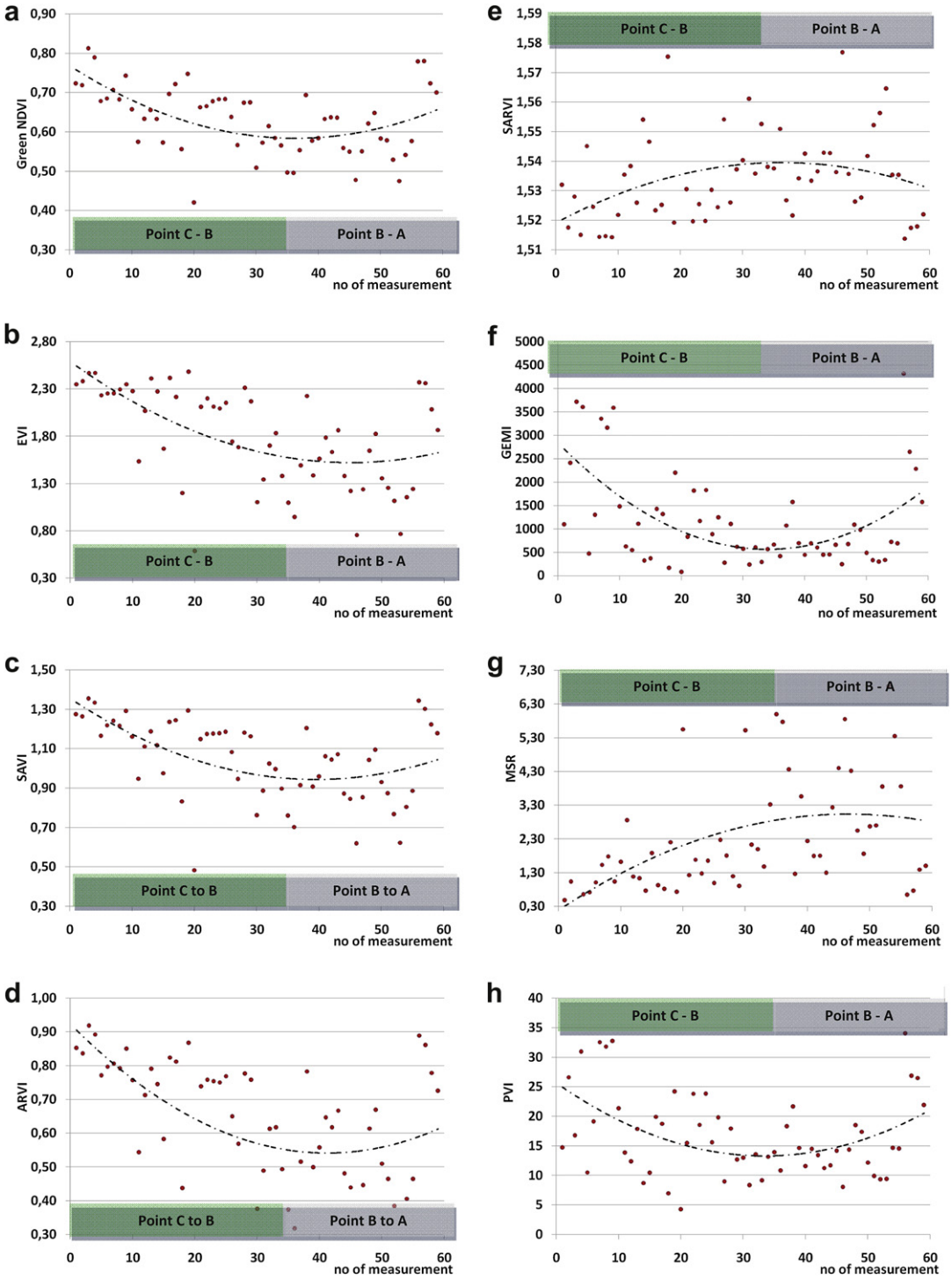

Fig. 13. Vegetation indices diagrams for the first section carried out in Nikaia 6 archaeological site. *X*-axis shows the number of measurements in each section while *Y*-axis indicated the index value as calculated for every measurement (a: Green NDVI, b: EVI, c: SAVI, d: ARVI, e: SARVI, f: GEMI, g: MSR, h: PVI). (For interpretation of the references to color in this figure legend, the reader is referred to the web version of this article.)

high (>0.8). The case is different in section c which is passing through the center of the magoula. Along this section, the topographic relief difference was most obvious moving from the top of magoula to the flat region. At the end of the magoula (Point *B*) the NDVI values are minimized while the same tendency is observed on the flat region of the parcel as well. Nevertheless, it should be noticed that the NDVI values are highest at the top of the magoula (Point *A*) in all three diagrams and while moving to the end of the magoula these tend to be slightly smaller.

Karatsantagli NDVI and SR diagrams (Fig. 11a–f) indicate that the magoula tends to have smaller NDVI values than the surrounding area (Points *B* and *B′*). This is obvious for sections a and b. The last section (c), which was taken at the southern part of the magoula, shows a non-significant difference of the NDVI profile. The top of the magoula (Point *A*) shows similar NDVI values with the flat regions of the parcel (Point *C*).

Section a of the Almyros II NDVI diagram (Fig. 12a) shows a slight difference of the NDVI profile canopy above and after the magoula.

Please cite this article in press as: Agapiou, A., et al., Observatory validation of Neolithic tells ("Magoules") in the Thessalian plain, central Greece, using hyperspectral spectroradiometric data, Journal of Archaeological Science (2012), doi:10.1016/j.jas.2012.01.001

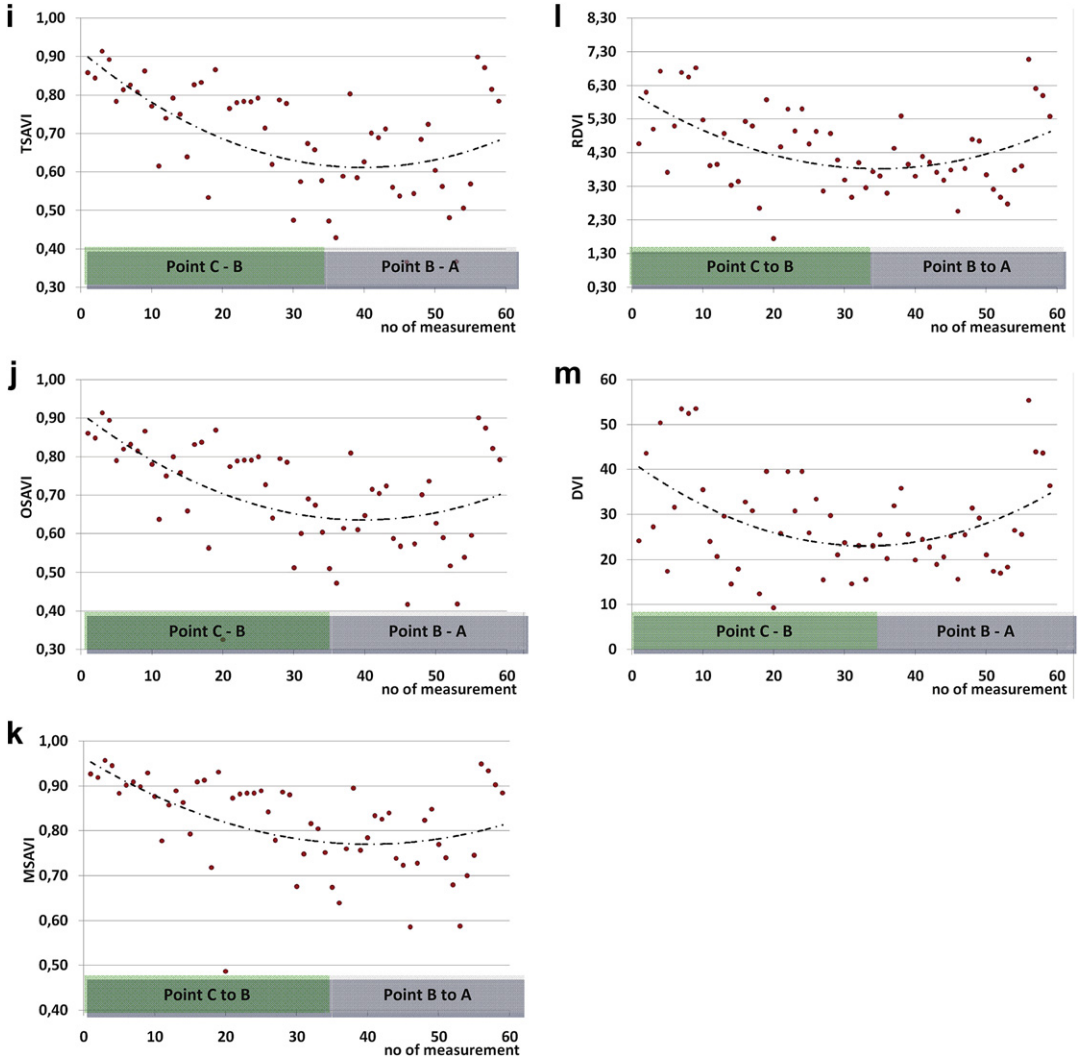

Fig. 14. Vegetation indices diagrams for the first section carried out in Nikaia 6 archaeological site. *X*-axis shows the number of measurements in each section while *Y*-axis indicated the index value as calculated for every measurement (i: TSAVI, j: OSAVI, k: MSAVI, l: RDVI, m: DVI).

This could be explained since this section (a) was taken just outside of the site. However, the other two sections (Fig. 12b and c) indicate high NDVI values over the magoula site (Point *A*) whereas the NDVI values tend to be smaller at the end of the magoula (Point *B*′). SR diagrams for sections b and c (Fig. 12e and f) show similar results as the NDVI plots. It is also interesting to examine section a (Fig. 12d) diagram since SR values are higher over the magoula (Point *A*) in comparison with the western end of the magoula (Point *B*′). This observation, as mentioned before, is not recorded from the NDVI diagram. SR index in this case is able to enhance the vegetation anomaly over the archaeological sites in contrast to the NDVI algorithm.

Further to NDVI and SR vegetation indices, more broadband vegetation indices (see Table 1) are presented in Figs. 13 and 14. These diagrams correspond to the first section of Nikaia 6. Similar outcomes were observed and for the rest sections of the archaeological sites examined in this study. The diagrams exhibit the same overall trend of data as those of NDVI and SR indices (Fig. 9a and d respectively). This comparison indicates that more broadband vegetation indices – further to NDVI and SR – may be used for the detection of archaeological sites, such as atmospheric and soil resistance indices. Especially the removal of atmospheric effects is very crucial when examine and analyze multi-temporal satellite images. Moreover GEMI (Fig. 13f) index seems to be able to enhance better the vegetation differences occurred in the healthy part of the parcel (Point *C*–*B*) compared to the lower relief of the magoula (Point *B*). However even simple indices such as SR or DVI tend to give similar results and to be able to detect archaeological sites.

Both similarities and disagreements between the vegetation indices and the spectral profiles of the sections can be found. This is due to the fact that spectral profiles were studied in a random sample selected for the aims of the papers. Nevertheless the similarities observed between indices and spectral profiles (e.g. section c, Nikaia 16) highlight that the latest may be used for the detection of archaeological sites. Detection of buried archaeological remains based on spectral profiles was shown by Agapiou et al. (2010).

6. Comparison with satellite imagery

A comparison between the results from the field campaigns and satellite imagery has been performed by the authors. A direct comparison between such data can highlight the benefits of ground spectroscopy for archaeological research as presented in this study. In this chapter the results from one archaeological site (Nikaia 6) are presented based on multispectral archive free distributed

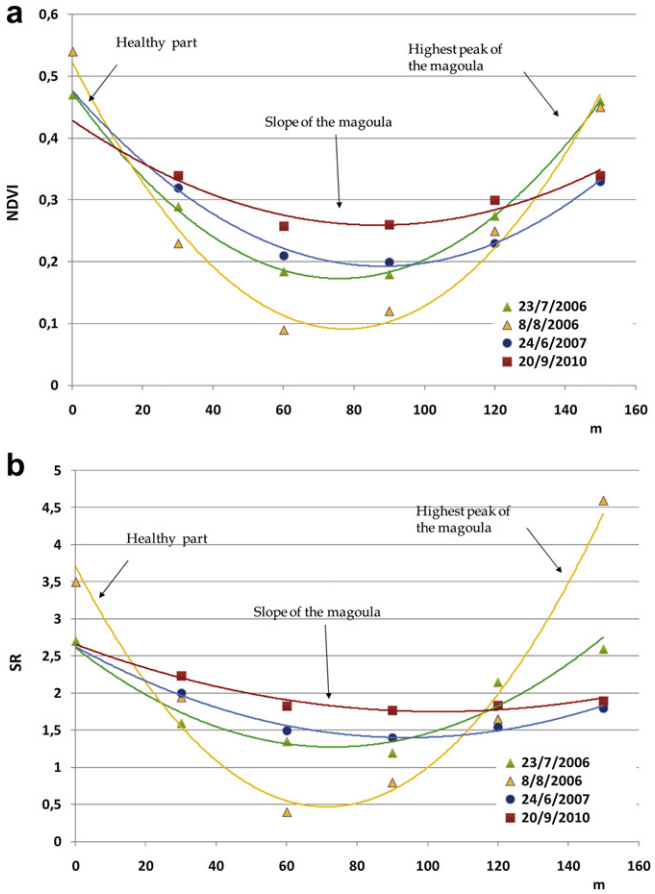

Fig. 15. NDVI (a) and SR (b) diagrams over Nikaia 6 for multi-temporal satellite images (3/07/2006; 08/08/2006; 24/06/2007 and 20/09/2010).

Landsat TM/ETM+ satellite images (23/07/2006; 08/08/2006; 24/06/2007 and 20/09/2010).

As it is shown in Fig. 15 the results derived from vegetation indices of Landsat TM/ETM+ images are similar with ground spectroradiometric measurements. Despite the medium spatial resolution of Landsat imagery, the characteristic curve of NDVI or SR (Fig. 15a and b respectively) is recorded for all images (multi-temporal). Therefore ground spectroscopy may be used either in order to detect the trend of archaeological sites before any satellite investigation (as presented in this paper) or the opposite one: to verify satellite investigation results (e.g. Agapiou and Hadjimitsis, 2011).

7. Conclusions

This paper presented the results of an extensive spectroradiometric survey over known archaeological sites. The case studies selected were four Neolithic settlements (magoules) located in Thessaly region in central Greece.

It was found out that the use of spectroradiometer can provide valuable information for identification of archaeological sites especially when it is combined with satellite imagery. Spectral profiles can be used as the first step in order to observe any significant differences of spectral response of the canopy in healthy vegetation sites and sites with archaeological interest. Using RSR filters, the narrow bands reflectance of spectroradiometer can be transformed into broadband reflectance for any satellite sensor (e.g. Landsat). Additionally, with the use of reflectance, vegetation indices can be calculated and validate the difference in spectral response over archaeological and non-archaeological sites.

Concerning the magoules, spectroradiometric measurements indicated that each magoula has its own spectral characteristics related to its own morphological characteristics. It was found out that the most promising results were extracted over the central section of each magoula while the other sections taken in a distance offset from the central one did not indicate any significant differences. The research proved that the highest peak of the magoula tends to give high NDVI and SR values (similar to the flat – healthy regions) while the slope of the magoula has lowest NDVI and SR values (and for the other indices as well). One explanation for this observation is based on the fact that top of the magoula seems to have similar hydrological behavior as the flat healthy region (e.g. same level of water surface run off and similar inclination ≈0%) in contrast to the slope of the magoula. The sloping part of the magoula seems to behave differently due to rainfall erosion processes. All these results denote the correlation between the morphology and the spectral response of canopy on the magoules.

Using this experience of the spectroradiometer, where ground hyperspectral data were collected, a researcher focusing in satellite imagery can seek and search for similarly spectral characteristics as those in the spectroradiometric campaign. The results from such investigation were presented in this paper. Indeed satellite images tend to give similar results as those of grounds spectroradiometric measurements for magoula Nikaia 6.

Ground spectroradiometric measurements can be used as an alternative approach in order to detect archaeological sites, since they can provide accurate spectral profiles for a wide spectral region. Anomalies of the crop spectral profiles due to archaeological sites can be recorded in detail and contribute to the construction of a predictive archaeological model in the future. However, the real benefit of this approach is when it is used in conjunction with satellite images.

As a follow up of the above research, the phenological cycle of several other crops will be monitored, using multispectral satellite images and ground spectroradiometric measurements in areas with archaeological interest.

Acknowledgments

These results are part of the PhD thesis of Mr. Athos Agapiou. The authors would like to express their appreciation to the Alexander Onassis Foundation for funding the PhD study. Thanks are given to the archaeologist Dr. Kostas Vouzaxakis for his valuable assistance during the field campaigns. Also thanks are given to the Remote Sensing Laboratory of the Department of Civil Engineering & Geomatics at the Cyprus University of Technology for the support (http://www.cut.ac.cy). Special thanks to the Cyprus University of Technology-Research Committee for their support.

Appendix. Supplementary material

Supplementary material associated with this article can be found, in the online version, at doi:10.1016/j.jas.2012.01.001.

References

Agapiou, A., Hadjimitsis, D.G., 2011. Vegetation indices and field spectroradiometric measurements for validation of buried architectural remains: verification under area surveyed with geophysical campaigns. Journal of Applied Remote Sensing 5, 053554–053561.

Agapiou, A., Hadjimitsis, G.D., Sarris, A., Themistocleous, K., Papadavid, G., 2010. Hyperspectral ground truth data for the detection of buried architectural remains. Lecture Notes of Computer Science 6436, 318–331.

Agapiou, A., Hadjimitsis, D.G., Papoutsa, C., Alexakis, D.D., Papadavid, G., 2011. The Importance of accounting for atmospheric effects in the application of NDVI and interpretation of satellite imagery supporting Archaeological Research: the case

studies of Palaepaphos and Nea Paphos Sites in Cyprus. Remote Sensing 3, 2605–2629. doi:10.3390/rs3122605.
Alexakis, A., Sarris, A., Astaras, T., Albanakis, K., 2009. Detection of neolithic settlements in Thessaly (Greece) through multispectral and hyperspectral satellite imagery. Sensors 9, 1167–1187.
Alexakis, A., Sarris, A., Astaras, T., Albanakis, K., 2011. Integrated GIS, remote sensing and geomorphologic approaches for the reconstruction of the landscape habitation of Thessaly during the neolithic period. Journal of Archaeological Science 38, 89–100.
Altaweel, M., 2005. The use of ASTER satellite imagery in archaeological contexts. Archaeological Prospection 12, 151–166.
Aqdus, S.A., Hanson, W.S., Drummond, J., 2007. A Comparative study for finding archaeological crop marks using airborne hyperspectral, multispectral and digital photographic data. In: Proceedings of the 2007, Annual Conference of the Remote Sensing and Photogrammetry Society. Newcastle University Oct. 11–15, 2009.
Aqdus, S.A., Drummond, J., Hanson, W.S., 2008. Discovering archaeological cropmarks: a hyperspectral approach. The International Archives of the Photogrammetry. Remote Sensing and Spatial Information Sciences XXXVII (Part B5).
Baret, F., Guyot, G., 1991. Potentials and limits of vegetation indices for LAI and APAR assessment. Remote Sensing of Environment 35 (2–3), 161–173.
Bassani, C., Cavalli, R.M., Goffredo, R., Palombo, A., Pascucci, S., Pignatti, S., 2009. Specific spectral bands for different land cover contexts to improve the efficiency of remote sensing archaeological prospection. The Arpi case study. Journal of Cultural Heritage 10, 41–48.
Campbell, J.B., 2002. Introduction to Remote Sensing London and New York.
Cavalli, R.S., Colosi, F., Palombo, A., Pignatti, S., Poscolieri, M., 2007. Remote hyperspectral imagery as a support to archaeological prospection. Journal of Cultural Heritage 8, 272–283.
Chen, J.M., 1996. Evaluation of vegetation indices and a modified simple ratio for boreal applications. Canadian Journal of Remote Sensing 22 (3), 229–242.
Galli, K.I., 1992. Atlas of Prehistoric Settlements of the Eastern Thessalian Plain. Thessaly Historical Research Center, Larissa, Greece (in Greek).
Gitelson, A.A., Kaufman, Y.J., Merzlyak, M.N., 1996. Use of a green channel in remote sensing of global vegetation from EOS-MODIS. Remote Sensing of Environment 58 (3), 289–298.
Glenn, E.P., Huete, A.R., Nagler, P.L., Nelson, S.G., 2008. Relationship between remotely-sensed vegetation indices, canopy attributes and plant physiological processes: what vegetation indices can and cannot tell us about the landscape. Sensors 8, 2136–2160.
Hadjimitsis, D.G., Themistocleous, K., Agapiou, A., Clayton, C.R.I., 2009. Multitemporal study of archaeological sites in Cyprus using atmospheric corrected satellite remotely sensed data. International Journal of Architectural Computing 7 (1), 121–138.
Huete, A.R., 1988. A soil-adjusted vegetation index (SAVI). Remote Sensing of Environment 25, 295–309.
Huete, A.R., Liu, H.Q., Batchily, K., van Leeuwen, W., 1997. A comparison of vegetation indices over a global set of TM images for EOS-MODIS. Remote Sensing of Environment 59, 440–451.
Jackson, R.D., Huete, A.R., 1991. Interpreting vegetation indices. Preventive Veterinary Medicine 11, 185–200.
Jordan, C.F., 1969. Derivation of leaf area index from quality of light on the forest floor. Ecology 50, 663–666.
Kaufman, Y.J., Tanré, D., 1992. Atmospherically resistant vegetation index (ARVI) for EOS-MODIS. IEEE Transactions on Geoscience and Remote Sensing 30, 261–270.
Lasaponara, R., Masini, N., 2005. QuickBird-based analysis for the spatial characterization of archaeological sites: case study of the Monte Serico Medioeval village. Geophysical Research Letter 32 (12), L12313.
Lasaponara, R., Masini, N., 2006. Identification of archaeological buried remains based on Normalized Difference Vegetation Index (NDVI) from Quickbird satellite data. IEEE Geoscience and Remote Sensing Letters 3 (3), 325–328.
Lasaponara, R., Masini, N., 2007. Detection of archaeological crop marks by using satellite QuickBird multispectral imagery. Journal of Archaeological Science 34, 214–221.
Lillesand, M., Kiefer, T., Chipman, J.W., 2004. Remote Sensing and Image Interpretation. Wiley International Edition.
Masini, N., Lasaponara, R., 2007. Investigating the spectral capability of QuickBird data to detect archaeological remains buried under vegetated and not vegetated areas. Journal of Cultural Heritage 8, 53–60.
Milton, J., 1987. Principles of field spectroscopy. Remote Sensing of Environment 8 (12), 1807–1827.
Negria, S., Leucci, G., 2006. Geophysical investigation of the Temple of Apollo (Hierapolis, Turkey). Journal of Archaeological Science 33 (11), 1505–1513.
Papadavid, G., Hadjimitsis, D.G., Themistocleous, K., Toulios, L., 2010. Spectral vegetation indices from field spectroscopy intended for evapotranspiration purposes for spring potatoes in Cyprus. SPIE 7824, 782410.
Parcak, S.H., 2009. Satellite Remote Sensing for Archaeology. Taylor and Francis Group Press, London and New York, Routledge.
Peddle, D.R., White, H.P., Soffer, R.J., Miller, J.R., LeDrew, E.F., 2001. Reflectance processing of remote sensing spectroradiometer data. Computers & Geosciences 27, 203–213.
Pinty, B., Verstraete, M.M., 1992. GEMI: a non-linear index to monitor global vegetation from satellites. Plant Ecology 101 (1), 15–20.
Qi, J., Chehbouni, A., Huete, A.R., Kerr, Y.H., Sorooshian, S., 1994. A modified soil adjusted vegetation index. Remote Sensing of Environment 48 (2), 119–126.
Richardson, A.J., Wiegand, C.L., 1977. Distinguishing vegetation from soil background information. Photogrammetric Engineering and Remote Sensing 43, 15–41.
Rondeaux, G., Steven, M., Baret, F., 1996. Optimization of soil-adjusted vegetation indices. Remote Sensing of Environment 55 (2), 95–107.
Roujean, J.L., Breon, F.M., 1995. Estimating PAR absorbed by vegetation from bidirectional reflectance measurements. Remote Sensing of Environment 51 (3), 375–384.
Rouse, J.W., Haas, R.H., Schell, J.A., Deering, D.W., Harlan, J.C., 1974. Monitoring the Vernal Advancements and Retrogradation (Greenwave Effect) of Nature Vegetation, NASA/GSFC Final Report Greenbelt.
Rowlands, A., Sarris, A., 2007. Detection of exposed and subsurface archaeological remains using multi-sensor remote sensing. Journal of Archaeological Science 34, 795–803.
Traviglia, A., 2005. Integration of MIVIS Hyperspectral remotely sensed data and Geographical Information Systems to study ancient landscape: the Aquileia case study. An International Journal of Landscape Archaeology 2, 139–170.
Tucker, C.J., 1979. Red and photographic infrared linear combinations for monitoring vegetation. Remote Sensing of Environment 8 (2), 127–150.
Ventera, M.L., Thompson, V.D., Reynoldsc, M.D., Waggoner, J.C., 2006. Integrating shallow geophysical survey: archaeological investigations at Totogal in the Sierra de los Tuxtlas, Veracruz, Mexico. Journal of Archaeological Science 33 (6), 767–777.
Vouzaksakis, C., 2009. Geographical Patterns and Theories of the Inter-settlement Space at Neolithic Thessaly, Unpublished Doctoral Dissertation, Aristotle University of Thessaloniki.
Wu, X., Sullivan, T.J., Heidinger, K.A., 2010. Operational calibration of the Advanced Very High Resolution Radiometer (AVHRR) visible and near-infrared channels. Canadian Journal of Remote Sensing 36 (5), 602–616.

Please cite this article in press as: Agapiou, A., et al., Observatory validation of Neolithic tells ("Magoules") in the Thessalian plain, central Greece, using hyperspectral spectroradiometric data, Journal of Archaeological Science (2012), doi:10.1016/j.jas.2012.01.001